

Hierarchical Control of Nanoparticle Deposition: High-Performance Electrically Conductive Nanocomposite Fibers via Infiltration

R. A. Vaia*

Air Force Materials Directorate,
Wright-Patterson Air Force Base, Ohio 45433

J. W. Lee

Syscom Technology, Inc., Hilliard, Ohio 43026

C. S. Wang, B. Click, and G. Price

University of Dayton Research Institute,
Dayton, Ohio 45469

Received March 24, 1998

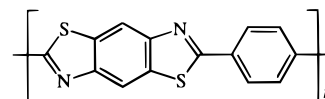
Revised Manuscript Received June 4, 1998

Twenty-first century space and aerospace technologies require the development of new lightweight inexpensive polymeric materials for applications that require tailored mechanical response as well as high electrical or thermal conductivity.¹ Nanostructured material systems^{2–6} offer a very promising alternative to conventional material options for these multifunctional applications. For polymeric-based nanocomposite systems, two general fabrication strategies have emerged: (a) controlled dispersion of preformed constituents, such as passivated nanoparticles⁷ or organically modified mica-type silicates,⁸ and (b) in situ chemical formation of the nanoscopic phase within or at interfaces (so-called templating), such as organized surfactant assemblies,⁹ block copolymers,^{7b,c,10} or porous and intercalated materials.^{8c,11} However, relatively few efforts^{12–14} have

been reported that attempted to control the chemical composition and shape as well as complex spatial distribution of the inorganic phase in the bulk. For applications that require connectivity or percolation of a secondary phase, such as electrical or thermal conductivity, spatial control of the distribution of the nanoscale constituents is critical on many length scales. For example, random percolation of conductive nanoparticles is not optional and results in unacceptably high loadings which adversely affect mechanical properties.^{15,16}

In this report we demonstrate in situ deposition of metal nanoparticles during wet-fiber spinning to form a connected, interpenetrated polymer–metal network parallel to the fiber axis which results in high-performance, highly conductive fibers. By considering the morphological development of the fiber during processing, spatial control of the metal deposition on a robust microfibrillar template may be achieved through controlled fiber swelling and infiltration of metal precursors and reduction agents.

Specifically, metal infiltrated polymer (MIP) fibers with conductivities exceeding 10⁴ S/cm are formed using wet-spinning of a lyotropic liquid crystalline solution of rigid-rod poly(*p*-phenylenebenzobisthiazole) (PBZT) in conjunction with precipitation of silver. PBZT is a member of the heterocyclic–aromatic rigid-rod^{17–19} and ladder²⁰ polymers which have been extensively examined for structural and optoelectronic applications.^{21–26}



Fibers are prepared by a coagulation process where the polymer is precipitated from a protic acid solution

* Corresponding author. Tel: 513-255-9184. E-mail: vaia@ml.wpafb.af.mil.

(1) *New World Vistas, Air and Space Power for the 21st Century*, USAF Scientific Advisory Board, US Air Force Office of Scientific Research: Bolling AFB, Washington DC.

(2) *Global Assessment of R&D Status and Trends in Nanoparticles, Nanostructured Materials, and Nanodevices*, International Technology Research Institute, Loyola College in Maryland: Baltimore, MD.

(3) Whiteside, G. M.; Mathias, J. P.; Seto, C. T. *Science* **1991**, *254*, 1312.

(4) Ozin, G. A. *Adv. Mater.* **1992**, *4*, 612.

(5) Godovski, D. Y. *Adv. Polym. Sci.* **1995**, *119*, 79.

(6) Philp, D.; Stoddart, J. F. *Angew. Chem., Int. Ed. Engl.* **1996**, *35*.

(7) For example see (a) Fendler, J. H. *Adv. Mater.* **1995**, *7*, 607 and references contained within. (b) Spatz, J. P.; Sheiko, S.; Möller, M. *Macromol.* **1996**, *29*, 3220. (c) Taleb, A.; Petit, C.; Pileni, M. P. *Chem. Mater.* **1997**, *9*, 950.

(8) For example, see: (a) Okada, A.; Usuki, A. *Mater. Sci. Eng. C*, **1995**, *3*, 109. (b) Vaia, R. A.; Ishii, H.; Giannelis, E. P. *Chem. Mater.* **1993**, *5*, 1694. (c) Giannelis, E. P. *Adv. Mater.* **1996**, *8*, 29 and references contained within.

(9) For example see (a) Bradley, J. S. *Clusters and Colloids, From Theory to Applications*; Schmid, G. Ed.; VCH Publications: New York, 1994. (b) Martino, A.; Yamanaka, S. A.; Kawola, J. S.; Loy, D. A. *Chem. Mater.* **1997**, *9*, 423 and references contained within. (c) Stockton, W.; Lodge, J.; Rachford, F.; Orman, M.; Falco, F.; Schoen, P. *J. Appl. Phys.* **1991**, *70*, 4679. (d) Pileni, M. P. *Langmuir* **1997**, *13*, 3266.

(10) For example see (a) Seregenia, M. V.; Bronstein, L. M.; Platonova, O. A.; Chernyshov, D. M.; Valetsky, P. M.; Hartmann, J.; Wenz, E.; Antonietti, M. *Chem. Mater.* **1997**, *9*, 923. (b) Sankaran, V.; Yue, J.; Cohen, R. E.; Schrock, R. R.; Silbey, R. J. *Chem. Mater.* **1993**, *5*, 1133. (c) Moffitt, M.; Eisenberg, A. *Chem. Mater.* **1995**, *7*, 1178 and 1185. (d) Ng Cheong Chan, Y.; Craig, G. S. W.; Schrock, R. R.; Cohen, R. E. *Chem. Mater.* **1992**, *4*, 885.

(11) For example, see: (a) Ogawa, M.; Kuroda, K. *Chem. Rev.* **1995**, *95*, 399. (b) Schollhorn, R. *Chem. Mater.* **1996**, *8*, 1747. (c) Hulteen, J. C.; Martin, C. R. *J. Mater. Chem.* **1997**, *7*, 1075.

(12) Krishnamoorti, R.; Giannelis, E. P. *Macromol.* **1997**, *30*, 4097.

(13) Ishizu, K.; Yamada, Y.; Saito, R.; Kanbara, T.; Yamamoto, T. *Polymer* **1993**, *34*, 2256.

(14) (a) Caplan, M. L.; Southward, R. E.; Thompson, D. W.; St. Clair, A. K. *Proc. Am. Chem. Soc., Div. Polym. Mater. Sci. Eng.* **1994**, *71*, 787. (b) Southward, R. E.; Thompson, D. W.; St. Clair, A. K. *Chem. Mater.* **1997**, *9*, 501.

(15) Stauffer, D.; Aharony, A. *Introduction to Percolation Theory*; Taylor & Francis: London, 1992.

(16) Sahimi, M. *Applications of Percolation Theory*; Taylor & Francis: London, 1994.

(17) Wolfe, J. R.; Loo, B. H.; Arnold, F. E. *Macromolecules* **1981**, *14*, 915.

(18) Adams, W. W.; Eby, R. K.; Mclemore, D. E. (Eds.) *Mater. Res. Soc. Symp. Proc.* **1988**, *134*.

(19) Fawaz, S. A.; Palazotto, A. N.; Wang, C. S. *Polymer* **1992**, *33*, 100.

(20) Jenekhe, S. A.; Tibbetts, S. T. *J. Polym. Sci.* **1988**, *B26*, 201. Jenekhe, S. A.; Johnson, P. O. *Macromolecules* **1990**, *23*, 4419.

(21) Mehta, R.; Lee, C. Y. *ACS Polym. Mater. Sci. Eng.* **1990**, *63*, 991.

(22) Lee, J. W.; Wang, C. S. *Polymer* **1994**, *35*, 3673.

(23) Prasad, P. N.; Williams, D. J. *Introduction to Nonlinear Optical Effects in Molecules and Polymers*; John Wiley: New York, 1991.

(24) Meredith, G. R.; VanDusen, J. G.; Williams, D. J. *Macromolecules* **1982**, *15*, 1385.

(25) Heeger, A. J.; Orenstein, J.; D. R. Ulrich (Eds.) *Nonlinear Optical Properties of Polymers. Mater. Res. Soc. Symp. Proc.* **1985**, *109*.

(26) S. Marder, R.; Sohn, J. E.; Sticky, G. D. (Eds.) *Materials for Nonlinear Optics Chemical Perspectives. Am. Chem. Soc. Symp. Ser.* **1991**, *455*.

by a nonsolvent, producing a wet fiber with a swollen microfibrillar network. The nanocomposite fibers were formed via infiltration of solubilized metal salts into an acid-swollen fiber, resulting in precipitation of insoluble precursor nanocrystals whose spatial distribution can be controlled by the rate of diffusion and solution concentration.^{27,28} Swelling and infiltration is general, applicable to various rigid-rod, semiflexible, or flexible polymers, and not restricted to special synthesis of metal-containing or complexing polymers. In contrast, the incorporation of solubilized metal precursors in the polymer solution^{14,29} prior to fiber spinning is restricted by the solubility of the precursor and the finite number of complexation sites. These limit total metal precursor loading and many times provide inadequate control of the final precursor distribution which is generally homogeneous.

The PBZT fibers were first prepared from a nematic liquid crystalline solution [13.7 wt % in polyphosphoric acid (PPA)] by conventional extrusion and coagulation in a 10 wt % phosphoric acid bath.³⁰ This process forms highly oriented fibers with a densely packed microfibrillar network, resulting from the mesostructure of the liquid crystalline solution.³¹ The wet-spun fiber was placed in an aqueous solution (30–70 wt %) of silver nitrate (Englehard Industries) at room temperature to allow silver ions to infiltrate the fiber. As indicated by the WAXD measurements, silver phosphate precipitated in the fiber due to the local silver and phosphate ion concentration exceeding their ionic product. Most importantly, the PBZT molecules were uniaxially oriented in the stretching direction and the orientation was not significantly altered by the incorporation of the silver phosphate.

Silver salts can be readily reduced to silver metal by chemical,^{29,33} thermal,¹⁴ or photo³⁴ reduction methods. In this study, the silver phosphate-containing fiber was briefly rinsed with deionized water and then placed in a 0.5 wt % sodium borohydride aqueous solution for up to 60 s to ensure complete reduction. Figure 1 shows the WAXD of the resulting silver-infiltrated fiber. The retention of equatorial reflections of the PBZT molecules

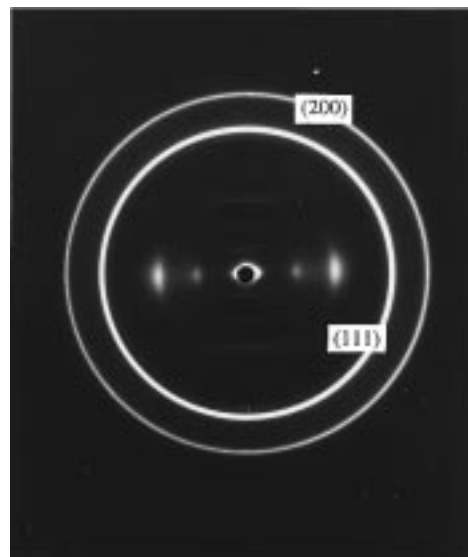


Figure 1. The wide-angle X-ray diffraction patterns of silver-infiltrated PBZT fiber.

indicates that the infiltration and reduction processes do not disrupt the uniaxial orientation of the polymer chains. Two strong X-ray reflections at the d spacing value of 2.04 and 2.36 Å correspond well to the characteristic (200) and (111) reflections of the face-center cubic silver crystalline structure. The absence of silver phosphate reflections indicates that the aqueous solution of sodium borohydride has diffused into the core of the fiber and completely reduced the silver salt. In fact, the majority of silver phosphate was readily converted to silver in less than 10 s. A simple Fickian model of diffusion into a cylinder of a diameter of 12 μm showed that significant accumulation of salt concentration in the core of the fiber occurs within 0.01 s using a diffusivity of 10^{-5} cm^2/s . The rapid process suggests that complete infiltration of a commercial fiber can be achieved in an in-line production process.

The silver-infiltrated fiber showed a distinct metallic luster in comparison to the otherwise dark brown PBZT control fiber. Scanning electron microscopy indicates that only a few isolated silver aggregates are present on the exterior of the fiber. Furthermore, the fiber appeared to maintain the similar surface contour of the control fiber. Figure 2 shows a bright field transmission electron micrograph of a microtomed (~ 90 nm) cross section of the fiber, indicating that the Ag nanoparticles were formed in the microfibrillar network as intended. With the aforementioned processing conditions, a thickness of 2–3 μm of dense silver deposition was observed near the fiber skin, whereas only a small amount of silver aggregates was present in the fiber core. The silver infiltration depth is fairly uniform around the fiber surface, regardless of the irregular surface contours. In general, the particles are elongated with 200–400 nm in the long axis and 50–100 nm in the short axis. Furthermore, a very thin layer of extremely fine silver particles on the order of 20 nm were observed right at the fiber surface. Coagulated rigid-rod fiber possesses a skin–core morphology in which the skin contains a much denser microfibrillar network than that of the core due to the coagulation process.³¹ In the skin region, the space between the microfibrils is smaller than that in the core area of the fiber. The morphologi-

(27) Lee, J. W.; Wang, C. S.; Vaia, R. A. US Patent Application Serial No. 60/071,779.

(28) Initial precipitation of a precursor salt is not necessary. A concentration gradient of solubilized precursor can be established by direct swelling of an initially unswollen polymer and subsequent reduction. Using variations of this infiltration processes, we have formed silver particles with average sizes as small as 7 nm in Kapton.

(29) (a) Yen, C.-C.; Huang, C.-J.; Chang, T.-C. *J. Appl. Polym. Sci.* **1991**, *42*, 439. (b) Huang, C.-J.; Yen, C.-C.; Chang, T.-C. *J. Appl. Polym. Sci.* **1991**, *42*, 2237. (c) Huang, C.-J.; Yen, C.-C.; Chang, T.-C. *J. Appl. Polym. Sci.* **1991**, *42*, 2267. (d) Yen, C.-C.; Huang, C.-J.; Chang, T.-C. *J. Appl. Polym. Sci.* **1992**, *46*, 1677.

(30) We used a 13.7 wt % PBZT/PPA solution that was homogenized in a Haake Rheomixer (model Rheocord 90) at 120 °C for 6 h, filtered, deaerated at 80 °C through a 74 μm stainless steel mesh, and extruded at 80 °C through a 0.010 in. spinneret into a single filament fiber by a dry-jet, wet-spinning process. The fiber was highly stretched during processing and a draw ratio of take-up speed to extrusion rate of about 60 was obtained.

(31) Cohen, Y.; Thomas, E. L. *Polym. Eng. Sci.* **1985**, *25*, 1093.

(32) Wide-angle X-ray diffraction (Cu $K\alpha$ radiation from a RU-200BVH Rigaku rotation anode operating at 40 kV and 200 mA monochromatized with graphite crystals). The scattering patterns were recorded on photographic films using an evacuated Statton camera with a camera length of 3 cm.

(33) Kurihara, L. K.; Chow, G. M.; Schoen, P. E. *Nanostruct. Mater.* **1995**, *5* (6), 607.

(34) Zhou, H. S.; Wada, T.; Sasabe, H.; Komiyama, H. *Synth. Met.* **1996**, *81*, 129.

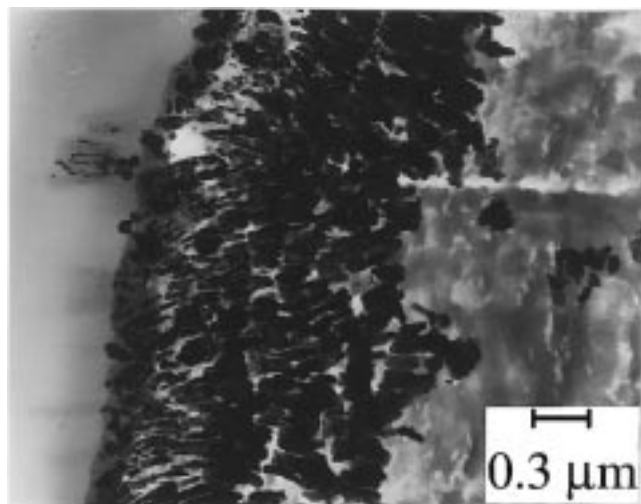


Figure 2. The transmission electron micrographs of the cross section of PBZT/Ag composite fiber that was prepared by infiltrating the PBZT fiber with 70 wt % silver nitrate solution and then reducing the silver salt to silver with 0.5 wt % sodium borohydride aqueous solution.

Table 1. Mechanical and Electrical Properties of PBZT Control Fiber and Silver Infiltrated Fiber

	modulus (GPa)	strength (GPa)	strain (%)	conductivity (S/cm)
PBZT control fiber	95.2	0.90	1.98	10^{-12} – 10^{-14}
PBZT/Ag composite fiber	51.8	1.05	3.29	2.5×10^4

cal distribution of the silver particles suggested that formation and networking of the silver nanoparticles were controlled by the robust PBZT fiber matrix template.

The electrical conductivity of the MIP fibers was determined by a two-point probe measurement on silver-reduced PBZT fibers that were subsequently rinsed in deionized water for 15 min and vacuum-dried for greater than 12 h. The infiltrated fiber was 40 μm in diameter and contained approximately 23 vol % silver. For the processing conditions discussed above, an optimal d.c. conductivity of 2.5×10^4 S/cm was obtained for the composite silver–PBZT fiber³⁵ (Table 1). This is 16 orders of magnitude greater than for the pristine fiber. In addition, even though the reactants are ionic, the electrical characteristics of the final washed and dried MIP fiber are overwhelmingly electronic. Ionic conductivity on the order of 10^{-1} S/cm is observed for wet fibers at intermediate processing steps, such as the initial protic acid swollen fiber. However, dried fibers at intermediate processing steps, such as the silver phosphate-containing fiber, exhibited conductivities less than 10^{-10} S/cm.

Because of the high thermooxidative stability of the PBZT base fiber, the electronic conductivity can be further enhanced by thermal annealing of the fiber

(35) For this processing methodology, fiber conductivities range from 10 to 10^4 S/cm.

under tension to improve the metal network. Additionally, since the metal is distributed within the microfibrillar matrix of the fiber, the metal/polymer interface adhesion is strongly enhanced by an interlocking mechanism. Twisting and bending of the fiber does not result in silver flaking and loss of electrical properties.

A major advantage of the rigid-rod heterocyclic fiber is its exceptional mechanical properties. The tensile strength of the commercially available rigid-rod PBO fiber is 23 times stronger than that of high-strength copper core (665 MPa). Preliminary tensile properties of current test PBZT fiber are listed in Table 1.³⁶ The MIP fibers are lighter weight and exhibit mechanical properties exceeding pure metal fibers. The tensile strength of the controlled PBZT base fiber (0.9 GPa) and silver-infiltrated PBZT composite fiber (1.05 GPa) are comparable, indicating that the fiber mechanical integrity was not affected by the silver infiltration and reduction process. The incorporation of the silver phosphate and silver particles presumably disrupts the packing efficiency of the PBZT microfibrillar network, reducing the fiber modulus ($\sim 46\%$ lower) while increasing the maximum strain ($\sim 66\%$ larger). Improvement of the silver-infiltrated fiber's modulus by heat treatment under tension and adaptation of a continuous fiber spinning process with silver infiltration and chemical reduction is currently under investigation.

By exploiting the morphological development during polymer processing, we have demonstrated a general procedure to control the secondary phase distribution in polymer hosts via controlled diffusion of precursor and template chemical reaction in confined areas within the polymer.^{27,37} It is hoped that such approaches will facilitate the extension of the unique properties of nanoscale materials from surface and thin film applications to multifunctional, bulk consolidated materials. By incorporating and subsequently reducing chemical precursors, whether metallic, ceramic, or polymeric, in a swollen microfibrillar network, high-performance composite fibers with embedded nanosized networks of functional secondary phases can be produced.

Acknowledgment. This work was partially supported by the Air Force Contract Numbers F33615-95-D-5044 and F33615-93-D-5326. The authors are grateful to Mrs. Pam Lloyd for preparing the TEM samples and Drs. George Slenski and Doug Dudis for many helpful discussions and encouragement.

CM9801845

(36) The fiber tensile modulus and strength were determined using an Instron Universal Testing Machine (model 1122) and fibers mounted on 1 in. paper tabs with fast setting epoxy. The fiber diameters were determined by using the Nikon Metaphot optical microscope. A series of tests was repeated in order to find out the consistent tensile stress required to rupture the fiber.

(37) Vaia, R. A.; Lee, J. W.; Click, W.; Price, G.; Wang, C. S. In *Organic/Inorganic Hybrid Materials*; Laine, R. M., Sanchez, C., Brinker, C. J., Giannelis, E. P., Eds.; MRS Proceedings Vol. 519, Pittsburgh, PA, 1998.